Hydrogen sites in amorphous $Pd_{85}Si_{15}H_x$ probed by neutron vibrational spectroscopy

1989 J. Phys.: Condens. Matter 1 1061

(http://iopscience.iop.org/0953-8984/1/6/004)

J. Phys.: Condens. Matter 1 (1989) 1061–1070. Printed in the UK

Hydrogen sites in amorphous $Pd_{85}Si_{15}H_x$ probed by neutron vibrational spectroscopy

J J Rush†, T J Udovic†, R Hempelmann‡, D Richter§ and G Driesen||

† Institute for Materials Science and Engineering, National Bureau of Standards, Gaithersburg, MA 20899, USA

‡ Los Alamos Neutron Scattering Center, Los Alamos National Laboratory, Los Alamos, NM 87545, USA

§ Institut Laue–Langevin, 38042 Grenoble Cédex, France

|| Institut für Festkörperforschung, Kernforschungsanlage Jülich, 517 Jülich, Federal Republic of Germany

Received 27 June 1988

Abstract. In order to clarify the discrepancy between the Gaussian distribution of H-site energies suggested from different macroscopic measurements and the evidence for two energetically well separated types of H sites obtained from a microscopic H diffusion study by means of quasi-elastic neutron scattering, we have measured neutron vibrational spectra of hydrogen in amorphous $Pd_{85}Si_{15}H_x$, $0.13 \leqslant x \leqslant 8.23$. At concentrations below 1% the spectra exhibit distinct features that indicate the occupation of distorted Pd_6 octahedra, along with a range of tetrahedral sites. These observations are consistent with a bimodal distribution of H-site energies in this glassy metal hydride.

1. Introduction

The binary Pd–Si phase diagram (Massalski 1986) exhibits a deep eutectic (810 °C) for $Pd_{84}Si_{16}$, so at about this composition metallic glasses can be prepared comparatively easily by rapid quenching from the melt. They readily absorb hydrogen and have thermodynamic and kinetic properties favourable for laboratory experiments. This is probably the main reason why $Pd_{1-y}Si_y/H$ is the most intensively investigated amorphous metal/hydrogen system and, in some sense, may now be considered as a prototype, as Pd/H is for binary metal/hydrogen systems.

The thermodynamics of hydrogen absorption in $Pd_{1-y}Si_yH_x$ was studied by electrochemical methods (Kirchheim *et al* 1982). The temperature and H concentration dependence of the resulting chemical potential was interpreted in terms of a Gaussian distribution of site energies. The temperature and H concentration dependence of the electrochemically determined H diffusion coefficient was also explained with the same set of microscopic parameters (Kirchheim 1982). Further support for the Gaussian model was obtained from high-pressure gas volumetric measurements (Baranowski 1984) which extended up to H_2 pressures of 20 kbar, corresponding to a H content of $Pd_{83}Si_{17}H_{50}$. Combined with Kirchheim's low-concentration electrochemical data, the chemical potential measured over four orders of magnitude in the fugacity could be described by a common set of microscopic parameters; this agreement is somewhat

0953-8984/89/061061 + 10 $02.50

surprising because the Gaussian model neglects H–H interactions that, without doubt, considerably contribute to the chemical potential at high hydrogen concentration. A continuous distribution of site energies has also been derived from a comparison of Gorsky and Snoek relaxation measurements (Berry and Pritchet 1981, 1983, 1986). On the other hand, Finocchiaro *et al* (1982) used a two-state model to describe their p–c–T data, but with little resonance in the scientific community.

A striking conclusion from a detailed microscopic study of the H diffusion in $Pd_{85}Si_{15}H_x$ by means of quasi-elastic neutron scattering (QNS) was the existence of two well separated timescales of hydrogen jump motion (Richter *et al* 1986). A semiquantitative interpretation of the neutron scattering data was possible in terms of a two-state diffusion-trapping model: the hydrogen atoms alternate between a 'mobile state', in which they propagate over the energetically unfavourable sites, and a 'trapped state', where the protons rest in low-energy trapping sites. Of course, the assumption of two discrete site energies is a crude approximation, and recent extended QNS investigations of the dependence on c_H and T of the H diffusion (Driesen 1987, Driesen *et al* 1989) instead provide evidence of two distributions of site energies (bimodal distribution). Although the QNS results revealed the existence of two separated classes of H jump rates, by their very nature they could not identify the two types of site involved.

The verification and identification of such a site distribution is the aim of the present neutron vibrational spectroscopy (NVS) study. This technique has successfully been applied to determine hydrogen sites close to trapping centres in refractory metals (Magerl *et al* 1983, Richter *et al* 1983) and in different intermetallic hydrides (Hempelmann *et al* 1984, 1989). For glassy metal hydrides, broad and featureless spectra were obtained, e.g. for $TiCuH_{0.93}$ (Rush *et al* 1980) and for $Ti_2NiH_{1.5}$ (Kai *et al* 1983), which were attributed to a broad distribution of hydrogen sites, mostly of tetrahedral type. Richards has connected the spread of the hydrogen site energies to the topological disorder in metallic glasses (Richards 1983). Therefore, our idea was that at very low hydrogen concentrations, when only the energetically lowest sites are occupied, the geometry of the occupied sites should be much more uniform, thus giving rise to better-structured neutron vibrational spectra. From these we attempt to extract structural information about the amorphous $Pd_{85}Si_{15}/H$ system.

2. Neutron vibrational spectroscopy

The capability of the otherwise widely used technique of neutron diffraction to determine hydrogen (deuterium) positions in metals is strongly diminished when the system of H sites to be investigated does not exhibit translational symmetry. In such a case, NVS can be a superior probe (Richter 1983, Hempelmann and Rush 1986). In § 2.1 we present the neutron scattering function. Unlike optical spectroscopic techniques, the NVS peak intensity is quantitatively proportional to the number of H atoms contributing. However, the detailed interpretation of neutron vibrational spectra requires a 'complete' scattering function, and therefore we include opto-acoustical and opto-optical two-phonon scattering processes. In § 2.2 we describe how we assign certain vibrational peaks to certain hydrogen sites by means of a simple lattice dynamical model.

2.1. Scattering function

Due to their light mass, hydrogen atoms occupying interstitial sites in metals undergo high-frequency optical vibrations which are superposed on the much slower and thus

energetically well separated acoustical vibrations of the host lattice. At low H concentrations, direct H–H interactions are negligible, and the hydrogen atoms may be considered as single independent three-dimensional Einstein oscillators, each with three vibrational degrees of freedom. Distributed over different types of sites, they independently contribute to the neutron scattering double-differential cross section:

$$\frac{\partial^2\sigma}{\partial\omega\partial\Omega} = \frac{\sigma^{\mathrm{tot}}}{4\pi}\frac{k_{\mathrm{f}}}{k_{\mathrm{i}}}N_{\mathrm{H}}\sum_{j=1}^{K} f_j S_j(Q,\omega) \tag{1}$$

where σ^{tot} is the total neutron cross section of hydrogen, k_{i} and k_{f} are the incident and final neutron wavenumbers, N_{H} is total number of H atoms in the beam and f_j the fraction of those occupying site j. At 80 K, the temperature of our experiment, the localised vibrations of each H site (henceforth, the subscript j is omitted) give rise to the following one-phonon scattering function for neutron energy loss:

$$S(Q,\omega) = \exp(-2W(Q))\sum_{i=1}^{3}\frac{\hbar^2Q^2}{6m_{\mathrm{H}}\hbar\omega_i}\delta(\hbar\omega-\hbar\omega_i). \tag{2}$$

Since we shall treat opto-acoustical sidebands explicitly, the (low-temperature) Debye–Waller factor describes the intensity damping both due to the localised modes and due to the band (acoustic-like) modes:

$$2W(Q) = \frac{\hbar^2Q^2}{6m_{\mathrm{H}}}\sum_{i=1}^{3}\frac{1}{\hbar\omega_i} + \frac{\hbar^2Q^2}{m_{\mathrm{M}}}\frac{3k_{\mathrm{B}}T}{k_{\mathrm{B}}^2\theta_{\mathrm{D}}^2}. \tag{3}$$

For the Debye temperature θ_{D} we use the value for Pd, in both (3) and (5). In the energy range of our experiment two kinds of two-phonon processes occur.

(i) The opto-acoustical scattering gives rise to sidebands at both sides of the optical peaks:

$$S^{\mathrm{oa}}(Q,\omega) = \exp(-2W(Q))\frac{\hbar^4Q^4}{12m_{\mathrm{M}}m_{\mathrm{H}}}\sum_{i=1}^{3}\frac{1}{\hbar\omega_i}Z(\omega-\omega_i)\frac{n(\omega-\omega_i)+1}{\hbar\omega-\hbar\omega_i}. \tag{4}$$

This equation takes into account the fact that for two-phonon neutron energy-loss scattering, the creation of an optical phonon is accompanied by both the creation and annihilation of an acoustical phonon; both processes are thermally weighted by means of the Bose factor $n(\omega-\omega_i)$. For the density of states (DOS) of the acoustic phonons we assume a Debye shape; so, per normal mode in (4), we take

$$Z(\omega) = (\hbar\omega)^2/(k_{\mathrm{B}}\theta_{\mathrm{D}})^3. \tag{5}$$

Equation (4) assumes further that the H atoms simply mirror the metal DOS, i.e., they follow the metal vibrations with the metal amplitude. As has been shown by Lottner *et al* (1979) this assumption is only a crude approximation, but it should suffice for a first-order correction.

(ii) The second harmonics (opto-optical two-phonon scattering) of our lowest-energy optical peaks still fall into the energy range of our spectra. Therefore, their scattering contribution has to be taken into account when the hydrogen occupancies of

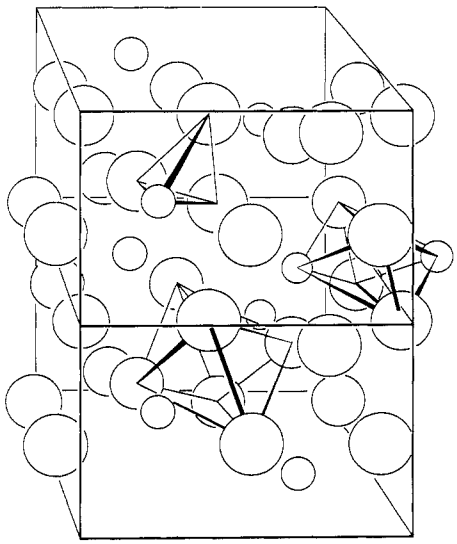

Figure 1. Two unit cells of the intermetallic compound Pd_3Si with three possible interstitial sites; instead of being positioned in the centre of the Pd_4Si_2 site, hydrogen could be displaced, thus occupying another Pd_3Si site (structural data from Villars and Calvert 1985).

different sites are evaluated from the respective peak intensities

$$S^{oo}(Q, \omega) = \exp(-2W(Q)) \sum_{i=1}^{3} \frac{\hbar^4 Q^4}{12 m_H^2 \hbar^2 \omega_i^2} \delta(\hbar\omega - 2\hbar\omega_i). \tag{6}$$

2.2. Frequency pattern

In glasses, the arrangement of atoms around a reference atom is not at all random, but almost analogous to that in crystals; the coordination number, nearest-neighbour distances, and bonding angles are determined by the chemical type of bonding and hence by the electronic structure of the atoms. In a metal–metalloid glass like $Pd_{1-y}Si_y$, the metalloid atoms exhibit a strong tendency to charge transfer and therefore are preferentially coordinated by metal atoms. The inter-atomic distances and the coordination numbers, determined for $Pd_{84}Si_{16}$ from a combination of neutron- and x-ray diffraction results (Sadoc and Dixmier 1977), agree well with the corresponding values of the intermetallic compound Pd_3Si, which exhibits the cementite Fe_3C structure. This structure can be regarded as regular packings of distorted trigonal prisms, each containing a Si atom. Actually, a model based on a random connection of trigonal prismatic units has been proposed for metal–metalloid glasses and allows an excellent description of the Si–Pd partial pair distribution function (Gaskell 1979, 1981, 1982). Therefore we assume, for the purpose of developing a model, that the structure of crystalline Pd_3Si (shown in figure 1) represents the local topology in amorphous $Pd_{85}Si_{15}$ reasonably well. We discern three different types of interstitial sites: a Pd_6 octahedral site, a Pd_4Si_2 octahedral site (both with point symmetry $\bar{1}$) and an approximately trigonal Pd_3Si site. The Pd_4Si_2 site is very anisotropic with two rather short (1.45 Å) and two rather long (2.52 Å) Pd–H distances. Hydrogen could also be displaced from the centre of this site into a more isotropic surrounding, thus forming the Pd_3Si^{II} tetrahedron mentioned in table 1.

With the following simple lattice dynamical model we are able to estimate the vibrational frequencies of hydrogen in these interstitial sites. For that purpose, the

Table 1. A comparison between the vibrational excitation energies (in meV) of H in amorphous $Pd_{85}Si_{15}$, predicted for different possible interstitial sites (see figure 1), and those resulting from least-squares fits to the neutron vibrational spectra; the resulting fractional intensities and the common linewidtdhs (in meV) are also listed.

	Prediction		
Site	$\hbar\omega_1$	$\hbar\omega_2$	$\hbar\omega_3$
Pd_6	63	66	70
Pd_3Si^I	98	101	135
Pd_4Si_2	46	90	97
Pd_3Si^{II}	96	101	137

	Experimental results							
	First site					Second site		
x in $Pd_{85}Si_{15}H_x$	$\hbar\omega_1$	$\hbar\omega_2$	$\hbar\omega_3$	HWHM	%	$\hbar\omega_1$	$\hbar\omega_2$	$\hbar\omega_3$
0.13	54(1)	65(2)	81(2)	7.3(12)	61	96(3)	111(3)	133(5)
0.27	56(2)	61(2)	76(2)	8.1(10)	53	95(2)	111(2)	134(3)
0.74	54(1)	63(1)	78(2)	8.5(8)	49	94(1)	114(1)	136(2)
2.14	51(1)	64(1)	77(1)	9.8(7)	47	93(2)	114(1)	134(2)
8.23	50(1)	63(1)	75(1)	11.3(10)	44	93(2)	115(1)	137(2)

eigenvalue problem

$$\mathbf{D}\hat{\boldsymbol{u}} = \omega^2\hat{\boldsymbol{u}} \tag{7}$$

has to be solved, where the eigenvectors $\hat{\boldsymbol{u}}$ indicate the directions of the vibrational displacement. To a good approximation we can take the metal–metalloid atoms as completely immobile; then $\mathbf{D}$ is a 3×3 dynamical matrix. The elements D_{ij} of this matrix represent the force acting on the hydrogen atom in the direction i, if it is displaced in the direction j. The force constants are generally expressed in terms of appropriate second derivatives of the potential. We take a simpler approach and model the restoring force $\boldsymbol{F}$ using longitudinal springs $\boldsymbol{s}^n = f^n\hat{\boldsymbol{s}}^n$ to the Z metal atoms of the first coordination shell (octahedron or tetrahedron):

$$\boldsymbol{F} = -\sum_{n=1}^{Z} f^n(\boldsymbol{u}\cdot\hat{\boldsymbol{s}}^n)\hat{\boldsymbol{s}}^n. \tag{8}$$

The unit vectors $\hat{\boldsymbol{s}}^n$ indicate the directions of the Z springs; their magnitude is given by the force constants

$$f^n = f^{\mathrm{M}}(r^n) = (c^{\mathrm{M-H}}/r^n)^2 \tag{9}$$

where r^n is the distance between the hydrogen atom and the metal atom n and where the force coefficients $c_{\mathrm{M-H}} = c^{\mathrm{Pd-H}}$ or $c^{\mathrm{Si-H}}$ (for hydrogen in $Pd_{1-y}Si_y$) characterise the hydrogen–metal–metalloid interaction. The $1/r^2$ dependence of f is chosen in order to model a $1/r$ dependence for the hydrogen frequencies. Such a dependence has been observed experimentally (Ross *et al* 1979) and has also been proposed on the basis of theoretical considerations (Sugimoto and Fukai 1981a, b). Simple algebra can be used

to transform (8) into the form of (7) with

$$D_{ij} = \sum_{n=1}^{Z} \hat{s}_i^n \hat{s}_j^n f^n. \tag{10}$$

This model, however, gives values for the frequencies for H in tetrahedral sites that are unreasonably low compared with frequencies for H in octahedral sites, because in the former case the restoring force and thus the hydrogen–metal interaction is modelled by two fewer springs than in the latter case. In order to compensate for this deficiency, we multiply the resulting tetrahedron frequencies by a factor $\frac{6}{4}$. This procedure is equivalent to multiplying the tetrahedral force constants by $\frac{6}{4}$ and is somewhat arbitrary. However, the frequency obtained is consistent with the value predicted for H hypothetically bound in a tetrahedral site in Pd from the curve of optical peak energy against hydrogen metal distance for FCC fluorite type hydrides (Ross *et al* 1979).

For the application of this model to H in c-Pd_3Si and thus to H in a-$Pd_{85}Si_{15}$ we need input values for the force coefficients. $c^{Pd-H} = 94.9$ meV Å^2 was calculated from the excitation energy $\hbar\omega = 69$ meV of H in Pd (Rush *et al* 1984). The (stretching) vibrational excitation energy of 250 meV for H in amorphous Si is known (Jones 1986), but it represents a covalent Si–H bonding, whereas we assume a dominantly metallic bonding in a-$Pd_{85}Si_{15}$; thus c^{Si-H} is not available *a priori* and was obtained by adjustment to our spectra. As will be discussed in § 5, we choose $c^{Si-H} = 127.2$ meV Å^2, so that 135 meV is obtained for the upper vibrational excitation energy of H in the Pd_3Si tetrahedron. The three predicted excitation energies for H in the different interstitial sites in a-$Pd_{85}Si_{15}$ are listed in the upper part of table 1.

3. Experimental details

The neutron scattering experiment was performed using the triple-axis spectrometer BT4 in its beryllium filter mode at the National Bureau of Standards research reactor. For the ambitious attempt of NVS on samples with less than 1% hydrogen, the outstandingly low background of this spectrometer turned out to be essential. The spectra were recorded for a constant number of monitor counts per data point with a counting sensitivity proportional to the reciprocal neutron velocity and, therefore, to $1/k_i$. Thus, the normalisation of the spectral data points to constant monitor counts compensates the k_f/k_i correction in (1) automatically during data acquisition.

About 50 g of amorphous $Pd_{85}Si_{15}$ were prepared by the melt-spinning technique (courtesy of Dr Kirchheim) in the form of thin ribbons (50–100 μm). The necessary compactness was achieved by pressing the ribbons into pellets. The cylindrical sample holder was attached to a liquid N_2 cryostat and was connected to a gas volumetric hydrogenation system via a capillary with a valve at the outlet of the cryostat. The sample was cooled down to 80 K and the background spectrum was taken (without hydrogen). Then the sample was heated up to 320 K and hydrogenated in the cryostat to the content $Pd_{85}Si_{15}H_{0.13}$. With the cryostat valve closed, the sample was again cooled down to 80 K. At this temperature, where the absorbed hydrogen is immobile, the hydrogen gas was pumped off from the sample holder in order to avoid gas scattering, and the first spectrum was taken. Afterwards the sample was heated up again, and the second hydrogen content $Pd_{85}Si_{15}H_{0.27}$ was established, and so on. The subsequent concentrations corresponded

to $Pd_{85}Si_{15}H_{0.74}$, $Pd_{85}Si_{15}H_{2.14}$, and $Pd_{85}Si_{15}H_{8.23}$. For this last concentration, the H_2 equilibrium pressure at 320 K amounted to 20 bar.

4. Results

The neutron vibrational spectra of $Pd_{85}Si_{15}H_x$ after background subtraction are displayed in figure 2. Tentatively we attribute the scattering intensity around 60 meV to the octahedral Pd_6 site and the scattering intensity in the 100–130 meV range to the tetrahedral Pd_3Si site. Therefore, we use (1) with two scattering functions and (2) for the quantitative data evaluation. We take a Gaussian lineshape, because it fits the data slightly better than a Lorentzian one. Each of the six Gaussians is associated with opto-acoustical sidebands according to (4); additionally we add second harmonics of the vibrational peaks of the first site according to (6). The resolution function is obtained by convoluting a Gaussian representing the monochromator crystal and a step function at 5.2 eV representing the Be filter. A convolution of the total scattering function with the resolution function was fitted to the data. The results are shown as full curves in figure 2. As starting values for the excitation energies, we took the predictions of table 1 for the Pd_6 and Pd_3Si^I sites. Since the sample induces background scattering, we allowed for a flat, energy-independent background in the fitting procedure. In order to stabilise the fit, it was necessary to restrict all Gaussians of a spectrum to one common (adjustable) linewidth. The parameters resulting from the fit are listed in the lower part of table 1. The total intensities and the sample-induced background levels are proportional to the hydrogen concentration, as shown in figure 3.

5. Discussion

Commencing with a *qualitative* consideration of the measured neutron vibrational spectra of hydrogen in amorphous $Pd_{85}Si_{15}$, we first notice that our spectra show structure, although this is less pronounced at our lowest and our highest concentration: at the lowest H concentration (about a tenth of a per cent!) the statistical scattering of the data points is large, whereas at the highest H concentration (nearly 10%) the vibrational peaks are already rather broad. The spectra generally exhibit two spectral ranges: a scattering maximum around 60 meV and scattering intensity in the 100–130 meV range. From experience with many other metal–hydrogen systems the former is attributed to hydrogen in octahedral type sites and the latter to hydrogen in 'tetrahedral' ones. We also see the tendency of the scattering intensity in the 100–130 meV range to increase with increasing hydrogen concentration.

For the *quantitative* data interpretation, the excitation energies of the Pd_6 octahedral sites were predicted using an externally available Pd–H force coefficient (see § 2.2). The experimental results for the first site are very close to these values as is shown in the comparison in table 1. Therefore, this class of sites is certainly dominated by Pd_6 octahedra. If the Pd_3Si site would have a trigonal point symmetry, it would give rise to a doubly degenerate hydrogen vibrational frequency, mainly determined by the Pd–H force constants, and a singlet, mainly representing the Si–H interaction. We observe such a pattern approximately and, therefore, associating the experimentally observed scattering intensity around 135 meV with the latter vibrations, we adapt the Si–H force coefficient so that our lattice dynamical model produces this excitation energy. With this

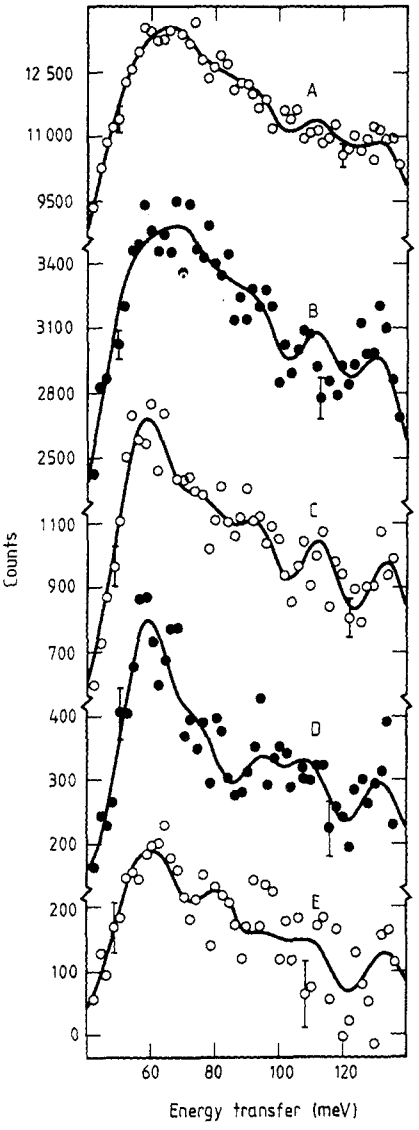

Figure 2. Neutron vibrational spectra of H in amorphous $Pd_{85}Si_{15}H_x$ at 80 K for x = (A) 8.23, (B) 2.14, (C) 0.74, (D) 0.27, (E) 0.13.

assumption, we obtain satisfactory agreement for the two other excitation energies of this site between our model and the observed spectral shape and intensity. Thus, the second class of sites is probably closely related to Pd_3Si tetrahedral sites. Our accuracy does not, however, allow us to distinguish between the different types of Pd_3Si sites listed in table 1. It is interesting that at 80 K, in spite of a hydrogen content as low as $Pd_{85}Si_{15}H_{0.13}$, at least two different types of interstitial sites appear to be occupied. Obviously, both sites exhibit a broad and overlapping distribution of site energies. Mixed site occupancies at high hydrogen concentrations have previously been suggested for a-$TiCuH_{0.93}$ (Rush *et al* 1980) and for $Ti_2NiH_{1.5}$ (Kai *et al* 1983); and also neutron vibrational spectra of a-$Zr_2PdD_{2.55}$ (Maeland *et al* 1987) exhibit scattering intensity in

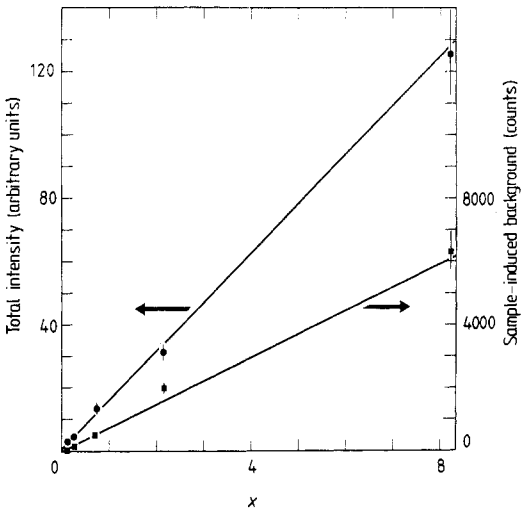

Figure 3. The hydrogen concentration dependence (x in $Pd_{85}S_{15}H_x$) of the parameters of total intensity and of sample-induced background resulting from the data fitting procedure.

the octahedral frequency range.

The model fits shown in figure 2 and table 1 are clearly consistent with the qualitative conclusions discussed above. Confidence in our overall quantitative evaluation of the neutron vibrational spectra is given by the reasonable concentration dependence of different quantities: the linewidth becomes broader with increasing H content and the relative occupancy of the first type of site decreases monotonically. But also important in our view is the linear increase of the total intensity and the sample-induced background, as shown in figure 3. On the other hand, while our model and fitting procedure provide results consistent with the data, we cannot claim uniqueness for the derived excitation energy and width parameters listed in table 1. What is clear is the existence of at least two different classes of occupied sites whose relative occupation is concentration dependent. From the observation of both types of sites at low H concentration at $T = 80$ K we conclude that the respective site energy distributions overlap in their low-energy wings. This result is not consistent with the assumption of a Gaussian distribution of hydrogen site energies (Kirchheim *et al* 1982), although this is certainly the simplest and most reasonable assumption for the interpretation of macroscopic data. However, it is generally not possible on the basis of such data to distinguish between such a simple site energy model and a more complex distribution such as that discerned in the present spectroscopic study.

In summary, the present NVS investigation has demonstrated the existence of a complex distribution of sites energies in amorphous $Pd_{85}Si_{15}H_x$ with at least two classes of occupied sites. An examination of the vibrational density of states over almost two orders of magnitude in H concentration (0.1–8.2%) shows that the relative occupation of different types of sites is concentration dependent. These results are consistent with previous QNS results which are interpreted in terms of a two-state diffusion–trapping model involving a bimodal distribution of site energies.

Acknowledgment

This work was partially supported by the Nato grant 86/0153.

References

Baranowski W 1984 *J. Less-Common Met.* **101** 115

Berry B S and Pritchet W C 1981 *Phys. Rev.* B **24** 2299

—— 1983 *Non-Traditional Methods in Diffusion* ed. G E Murch, H K Birnbaum and J R Cost (Philadelphia: The Metallurgical Society of the American Institute of Mining, Metallurgical and Petroleum Engineers) p 83

—— 1986 *Hydrogen in Disordered and Amorphous Solids* (Nato ASI Series B, vol 136) ed. G Bambakidis and R C Bowman (New York: Plenum) p 215

Driesen G 1987 *PhD Thesis* Universities of Antwerpen and Julich

Driesen G, Hempelmann R, Richter D and Coddens G 1989 unpublished

Finocchiaro R S, Tsai C L and Giessen B L 1982 *Proc. Rapidly Solidified Amorphous and Crystalline Alloys* ed. B H Kear, B C Giessen and M Cohen (Amsterdam: Elsevier) p 23

Gaskell P H 1979 *J. Non-Cryst. Solids* **32** 207

—— 1981 *Nature* **289** 474

—— 1982 *Proc. 4th Int. Conf. Rapidly Quenched Metals (Sendai)* ed. T Masumoto and K Suzuki (Sendai: Japan Institute of Metals) p 247

Hempelmann R, Richter D, Eckold G, Rush J J, Rowe J M and Montoya M 1984 *J. Less-Common Met.* **104** 1

Hempelmann R, Richter D, Hartmann O, Karlsson E and Wäppling R 1989 *J. Chem. Phys.* at press

Hempelmann R and Rush J J 1986 *Hydrogen in Disordered and Amorphous Solids* (Nato ASI Series B, vol 136) ed. G Bambakidis and R C Bowman (New York: Plenum) p 283

Jones B L 1986 *Hydrogen in Disordered and Amorphous Solids* (Nato ASI Series B, vol 136) ed. G Bambakidis and R C Bowman (New York: Plenum) p 51

Kai K, Ikeda S, Fukunaga T, Watanabe N and Suzuki K 1983 *Physica* B **120** 342

Kirchheim R 1982 *Acta Metall.* **30** 1069

Kirchheim R, Sommer F and Schluckebier 1982 *Acta Metall.* **30** 1059

Lottner V, Schober H R and Fitzgerald W J 1979 *Phys. Rev. Lett.* **52** 1163

Maeland A J, Lukacevick E, Rush J J and Santoro A 1987 *J. Less-Common Met.* **129** 77

Magerl A, Rush J J, Rowe J M and Wipf H 1983 *Phys. Rev.* B **1** 6927

Massalski T B (ed.) 1986 *Binary Alloy Phase Diagrams* vol 2 (Metals Park, OH: American Society for Metals)

Richards P M 1983 *Phys. Rev.* B **27** 2059

Richter D 1983 *Springer Tracts in Modern Physics* vol 101 (Berlin: Springer)

Richter D, Driesen G, Hempelmann R and Anderson I S 1986 *Phys. Rev. Lett.* **57** 731

Richter D, Rush J J and Rowe J M 1983 *Phys. Rev.* B **27** 6227

Ross D K, Martin P F, Oates W A and Khoda Bakhsh R 1979 *Z. Phys. Chem., NF* **114** 221

Rush J J, Rowe J M and Maeland A J 1980 *J. Phys. F: Met. Phys.* **10** L283

Rush J J, Rowe J M and Richter D 1984 *Z. Phys.* B **55** 283

Sadoc J F and Dixmier J 1977 *The Structure of Non-Crystalline Materials* ed. P H Gaskell (London: Taylor and Francis) p 85

Sugimoto H and Fukai Y 1981a *J. Phys. Soc. Japan* **51** 2554

—— 1981b *J. Phys. F: Met. Phys.* **11** L137

Villars P and Calvert L D (ed.) 1985 *Pearson's Handbook of Crystallographic Data for Intermetallic Phases* vol 3 (Metals Park, OH: American Society for Metals)